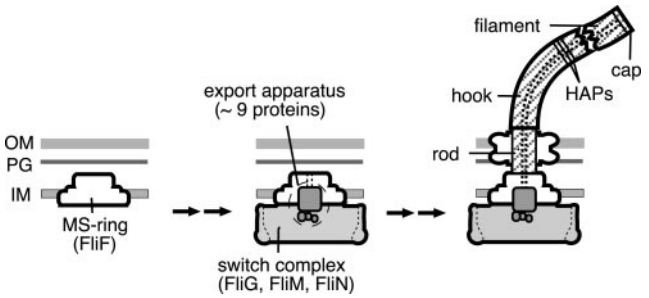

FIG. 1. Simplified flagellar assembly scheme. The arrows represent many assembly steps that are omitted for simplicity. The switch complex and the export apparatus are assembled at about the same time, relatively early in flagellar assembly. The export apparatus transports the components that form the exterior axial structures (the rod, hook, hook-associated proteins, and filament [cross-hatched]) into a central channel that traverses the length of the flagellum, indicated by the dashed lines. IM, inner membrane; PG, peptidoglycan; OM, outer membrane; HAPs, hook-associated proteins.

sembled, but their rotation is slow and irregular (65). These observations suggest that incomplete C rings are sufficient for flagellar assembly but cannot support normal motor rotation. The C-terminal parts of FliN (residue ~58 to the end) are best conserved and most important for function; a FliN fragment lacking 57 N-terminal residues supported swarming motility at about one-third the wild-type rate (65).

The molecular mechanisms of motor rotation, CW-CCW switching, and flagellar export are not understood, mainly due to a lack of structural information. Structures are known for relatively few flagellar proteins and for none of the export apparatus proteins except the chaperone FliS (15). To provide a structural basis for understanding the functions of FliN, we solved its structure by X-ray crystallography and studied its state of association by analytical ultracentrifugation. A stable complex of FliN with FliM was also characterized. The data obtained lead to a model for the structure of the C ring and highlight the functional importance of a prominent hydrophobic patch on the surface of FliN.

MATERIALS AND METHODS

Cloning and protein expression. The *Thermotoga maritima* homolog of *fliN* was identified first by a BLAST search of the unpublished genome data and then from the published genome sequence. In certain (mainly gram-positive) species the FliN homolog has additional N-terminal parts that make it about twice as large as it is in other species, and it is designated FliY (7). The *T. maritima* genome encodes two proteins (designated FliY-1 and FliY-2 in the annotated sequence) that together resemble FliY. The second of these is the homolog of FliN and was the subject of the present study. Constructs encoding residues 23 to 154 of *T. maritima* FliN and full-length *T. maritima* FliM were obtained by PCR amplification of genomic DNA (a gift from R. Huber, University of Regensburg). Primer sequences for PCR were based on the *T. maritima* genome sequence (53). *T. maritima* FliN is predicted to have 154 residues on the basis of the genome sequence (53). The *T. maritima* FliN protein studied here is a 132-residue construct that lacks 22 residues from the N terminus but encompasses the parts found to be essential in *Escherichia coli* (65), and its size is similar to that of the *E. coli* protein (137 residues). The constructs were cloned into the NdeI and BamHI sites of the vector pSBETa for *fliN* (58) or pAED4 for *fliM* (13).

Either the FliN protein alone or FliN and FliM together were overexpressed in BL21(DE3) cells (61). The cells were grown overnight at 37°C to an optical density at 600 nm of approximately 1.5 and then induced with 0.6 mM isopropyl-β-D-thiogalactopyranoside (IPTG) for 3 h. The cells were collected by centrifugation, frozen in liquid nitrogen, and stored at −70°C.

Protein purification. Frozen cells were thawed and resuspended in lysis buffer (50 mM Tris-HCl [pH 8.0], 5 mM EDTA), and protease inhibitors were added at the following concentrations: phenylmethylsulfonyl fluoride, 170 μg/ml; pepstatin A, 0.7 μg/ml; leupeptin, 0.5 μg/ml; and aprotinin, 2 μg/ml. The cells were sonicated, passed through a French pressure cell, sonicated again, and then centrifuged at 20,000 × *g* for 30 min at 4°C. The cold supernatant was mixed with 3 volumes of boiling lysis buffer and kept at 85°C for 15 min. The lysate was cooled in an ice-water bath, and the denatured proteins were pelleted by centrifugation at 100,000 × *g* for 1 h at 4°C.

For purification of FliN, a saturated $(NH_4)_2SO_4$ solution was added to the clarified lysate (~200 ml) to obtain a final $(NH_4)_2SO_4$ concentration of 0.5 M, and the solution was loaded onto a phenyl-Sepharose hydrophobic affinity column (Pharmacia) equilibrated in 50 mM Tris-HCl (pH 8.0)–0.5 M $(NH_4)_2SO_4$–5 mM EDTA. The column was washed with the same buffer until the UV trace returned to the baseline (~500 ml). Proteins were eluted from the column in 50 mM Tris-HCl (pH 8.0)–0.15 M $(NH_4)_2SO_4$–5 mM EDTA. Fractions containing FliN were pooled, dialyzed, concentrated by ultrafiltration, and loaded onto a Superdex-200 size exclusion column (Pharmacia). The column was run in 50 mM Tris-HCl (pH 8.0)–200 mM NaCl. Fractions containing FliN were pooled and concentrated by ultrafiltration.

For purification of FliM plus FliN, clarified lysate (typically ~200 ml) was loaded directly onto a Q-Sepharose column (Pharmacia), which was washed with ~500 ml of 50 mM Tris-HCl (pH 8.0) and then developed with a 0 to 1 M NaCl gradient in the same buffer. The FliM and FliN proteins eluted together; fractions containing the proteins were pooled, and saturated $(NH_4)_2SO_4$ was added to obtain a final $(NH_4)_2SO_4$ concentration of 0.5 M. The solution was loaded onto a phenyl-Sepharose column equilibrated in 50 mM Tris-HCl (pH 8.0)–0.5 M $(NH_4)_2SO_4$, and proteins were eluted with a 0.5 to 0 M $(NH_4)_2SO_4$ gradient. Fractions containing FliM plus FliN were pooled, concentrated by ultrafiltration, and loaded onto a Superdex-200 column. The column was run in 50 mM Tris-HCl (pH 8.0)–200 mM NaCl. Fractions containing FliM plus FliN were identified by Coomassie blue-stained sodium dodecyl sulfate-polyacrylamide gel electrophoresis (SDS-PAGE), pooled, and concentrated by ultrafiltration.

The *E. coli* FliN studied here was the full-length protein and was purified as described previously (54).

Analytical ultracentrifugation. For analytical ultracentrifugation experiments we used the proteins described above (full-length *E. coli* FliN, residues 23 to 154 of *T. maritima* FliN, and full-length *T. maritima* FliM). Sedimentation equilibrium experiments were conducted at 20°C with a Beckman Optima XL-A analytical ultracentrifuge by using an AnTi60 rotor with six-channel, 12-mm-thick, charcoal-Epon centerpieces. Three channels contained protein samples at different concentrations, and three channels contained buffer in dialysis equilibrium with the protein solution for use as optical references. The buffer was 50 mM Tris (pH 8.0)–200 mM NaCl. The FliN concentration ranged from 0.5 to 2 μM (on a monomer basis), and the concentration of FliM plus FliN ranged from 0.05 to 0.2 μM (total subunit concentration).

Samples were centrifuged until sedimentation equilibrium and chemical equilibrium were attained. Absorbance data were taken at 0.001-cm intervals and were averages of 10 measurements. Absorption measurements were obtained at 230 nm. The approach to equilibrium was monitored by comparison of scans taken at 4-h intervals. Partial specific volumes were calculated for each protein from the amino acid sequence, resulting in the following values: *E. coli* FliN, 0.7368 ml/g; *T. maritima* FliN, 0.7578 ml/g; and *T. maritima* FliM, 0.7443 ml/g. The buffer density was calculated and corrected for temperature by using the method of Laue et al. (39), which resulted in a value of 1.0079 g/ml at 20°C. A 360-nm scan was used to check for anomalous light bending in the 230-nm scan and to define the range of usable data.

Plots of absorbance versus radial distance were fitted by nonlinear regression by using the ORIGIN software package (Microcal Software) and an additional module supplied by Beckman Instruments. Data obtained from the different loading concentrations and from different rotational speeds (when applicable) were analyzed simultaneously. The fits incorporated a baseline offset to account for the zero offset of the optical system or the presence of any absorbing, nonsedimenting components. Initial estimates of the baseline offset term were obtained by overspeeding the sample at the completion of the run to deplete the meniscus of solute.

Velocity-sedimentation experiments were carried out with the XL-A ultracentrifuge with an AnTi60 rotor at 20°C by using double-sector centerpieces. A protein sample (300 to 400 μl) was added to one channel, and buffer was added to the reference compartment. Absorbance data were acquired at 280 nm with radial increments of 0.002 cm in continuous-scanning mode. The rotational velocity for all three proteins was between 35,000 and 45,000 rpm. Scans were taken at 2-min intervals. The sedimenting boundaries were fitted to a model